Limnol. Oceanogr., 56(4), 2011, 1330–1342
© 2011, by the American Society of Limnology and Oceanography, Inc.
doi:10.4319/lo.2011.56.4.1330

Increase in Rubisco activity and gene expression due to elevated temperature partially counteracts ultraviolet radiation–induced photoinhibition in the marine diatom *Thalassiosira weissflogii*

E. Walter Helbling,[a,*] Anita G. J. Buma,[b] Peter Boelen,[b] Han J. van der Strate,[b] M. Valeria Fiorda Giordanino,[a] and Virginia E. Villafañe[a]

[a] Estación de Fotobiología Playa Unión and Consejo Nacional de Investigaciones Científicas y Técnicas, Casilla de Correos No. 15 Rawson, Chubut, Argentina

[b] Department of Ocean Ecosystems, Energy and Sustainability Research Institute Groningen, University of Groningen, The Netherlands

Abstract

We performed outdoor experiments to evaluate the effect of temperature on photoinhibition properties in the cosmopolitan diatom *Thalassiosira weissflogii*. Cultures were exposed to solar radiation with or without ultraviolet radiation (UVR, 280–400 nm), UV-A (320–400 nm), and UV-B (280–320 nm) at both 20°C and 25°C. Four possible cellular mechanisms involved in UVR stress were simultaneously addressed: carbon incorporation, chlorophyll *a* fluorescence of photosystem II, xanthophyll cycle activity, and ribulose-1,5-biphosphate carboxylase : oxygenase (Rubisco) activity and gene expression. Experiments consisted of daily cycles (i.e., the daylight period) and short-term incubations (i.e., 1 h centered on local noon). Samples incubated at 25°C had significantly less UVR-induced inhibition of carbon fixation and effective photochemical quantum yield compared to those incubated at 20°C. At 25°C Rubisco activity and gene expression were significantly higher than at 20°C. The higher Rubisco activity and gene expression were correlated with less dissipation of excess energy, evaluated via non-photochemical quenching, and the de-epoxidation state of the xanthophyll pigments, as more photons could be processed. An increase in temperature due to climate change would partially counteract the negative effects of UVR by increasing the response of metabolic pathways, such as those involved in Rubisco. This, in turn, may have important consequences for the ecosystem, as higher production (due to more Rubisco activity) could be expected under a scenario of global warming.

Marine phytoplankton are responsible for about 40% of global primary productivity (Behrenfeld et al. 2006) through the process of photosynthesis. In addition to their notable importance as primary producers, phytoplankton also have a key role in taking up the excess carbon that has been released from anthropogenic activities since the time of the Industrial Revolution (Beardall et al. 2009). There is, therefore, an obvious interest in assessing the relative importance of the factors that affect physiological characteristics as well as the possible effects of climate change upon these organisms.

One of the factors that affect phytoplankton photosynthesis is ultraviolet radiation (UVR, 280–400 nm). Increased interest in UVR-driven effects has occurred since the discovery of the ozone 'hole' over the Antarctic continent (Farman et al. 1985), with the concomitant increase in the most energetic waveband (i.e., UV-B [280–315 nm]). Since then, a vast body of literature has been produced with regard to the effects of UV-B on polar phytoplankton photosynthesis (*see* review by Vernet and Smith [1997]). More recently, though, it has been recognized that natural levels of UVR cause significant effects with regard to phytoplankton photosynthesis around the globe (*see* reviews by Villafañe et al. [2003] and by Häder et al. [2007]). Yet phytoplankton may respond to UVR to various degrees based on their specific sensitivity and their potential to photoacclimate.

* Corresponding author: whelbling@efpu.org.ar

Most studies addressing the effects of UVR on phytoplankton photosynthesis have focused on carbon incorporation or oxygen evolution, many of which demonstrate the relative importance of UV-A (315–400 nm) in causing photoinhibition (reviewed by Villafañe et al. 2003). Other studies have focused on the effects of UVR on the reaction center of photosystem II (PSII). Measurements of chlorophyll *a* (Chl *a*) fluorescence of PSII in phytoplankton have demonstrated a classical response of inhibition of the PSII yield under exposure to photosynthetic active radiation (PAR, 400–700 nm), a response that is generally further reduced by UVR. These responses are typically followed by partial or complete recovery once the stress is removed (Villafañe et al. 2007; Roncarati et al. 2008; Halac et al. 2009). To minimize the damage produced on PSII, phytoplankton deploy a suite of mechanisms that can adjust photosynthesis on short time scales (seconds to minutes), such as the xanthophyll cycle (Olaizola and Yamamoto 1994; Dubinsky and Stambler 2009; Van De Poll et al. 2010), although the effectiveness of the xanthophyll cycle under high UVR levels is under debate (Van De Poll and Buma 2009). In addition, state transitions (reversible phosphorylation-mediated antenna size reduction of PSII by redistribution of energy to PSI) may occur, thereby contributing to non-photochemical fluorescence quenching (NPQ; Finazzi et al. 2006). Only a few UVR studies have focused on particular key enzymes associated with carbon acquisition, such as ribulose-1,5-biphosphate carboxylase : oxygenase (Rubisco). Lesser et al. (1996)

found a significant reduction in the total Rubisco pool of natural Antarctic phytoplankton when samples were exposed to UVR; such a reduction was also found for the dinoflagellate *Prorocentrum micans* (Lesser 1996*a*). Bouchard et al. (2008) found a reduced abundance of the large subunits of Rubisco in phytoplankton subjected to nutrient limitation and supplemental UV-B as well as exacerbated photoinhibition, as compared to phytoplankton exposed to ambient surface irradiance.

While there is a negative effect of UVR on the photosynthetic process, the interaction of this variable with others can alter the overall picture, as some variables can act synergistically or antagonistically (Dunne 2010). For example, in cultures exposed to UVR, nutrient addition resulted in higher effective photochemical quantum yield as compared to non-enriched cultures (Marcoval et al. 2007). Studies carried out by Gao et al. (2009) indicated that enhanced CO_2 concentrations exacerbated UVR stress on photosynthesis of calcified organisms; however, Sobrino et al. (2005) found opposite results when evaluating the photosynthesis of two species of *Nannochloropsis*. Temperature is also a variable that can considerably influence UVR responses in phytoplankton. In particular, elevated temperature seems to ameliorate UVR-induced stress (Sobrino and Neale 2007; Halac et al. 2010) and is suggested to be related to enhanced enzymatic conversion of xanthophyll cycle pigments (Demming-Adams and Adams 1992), the potential enhancement of Rubisco activity, and to enhanced D1 repair (Bouchard et al. 2006). A recent study (Halac et al. 2010) showed the responses of two marine diatoms (*Chaetoceros gracilis* and *Thalassiosira weissflogii*) exposed to UVR and elevated temperature using pulse amplitude modulated (PAM) fluorescence techniques. The authors concluded that increased temperature benefited *C. gracilis* by decreasing photoinhibition via dissipation of excess energy (NPQ). However, this process, although measurable, was much less significant in *T. weissflogii*, and therefore it did not fully explain the variability observed in the effective photochemical quantum yield in this species.

The temperature dependence of physiological changes under UVR stress is of special interest in the context of global change. For this reason, the aim of the present study was to thoroughly evaluate the physiological background of the temperature dependence of natural UVR stress on photosynthesis in the cosmopolitan diatom *T. weissflogii* (Grunow) G. Fryxell & Hasle. To this end, we simultaneously addressed four possible cellular mechanisms involved in UVR stress: carbon incorporation, Chl *a* fluorescence of PSII, xanthophyll cycle activity, and Rubisco activity and gene expression. To the best of our knowledge, this study represents the first in which four cellular 'targets' are simultaneously considered under natural solar conditions in order to understand the UVR effect from the 'light cycle' (antennae) to the 'dark reactions' (Calvin–Benson cycle).

Methods

Culture conditions and study area—T. weissflogii (Grunow) G. Fryxell & Hasle (Microalgal Culture Collection, Estación de Fotobiología Playa Unión [EFPU], Argentina) was grown in 4-liter Erlenmeyer flasks (UV opaque) in f/2 medium (Guillard and Ryther 1962) with a photoperiod of 12 : 12-h light : dark in two growth chambers (Sanyo model ML 350 and Minicella) at different temperatures: Prior to the outdoor exposures, cultures were acclimated for 2 weeks to 20°C or 25°C at a saturating irradiance of 235 μmol quanta m^{-2} s^{-1} (51 W m^{-2}) of PAR. We used this PAR level during the acclimation period because it was previously determined by us to be above the saturation light value (I_k) (V. E. Villafañe unpubl.). Nevertheless, in the water column, cells would experience irradiance above and below that level, depending not only on the position of the cells in the water column but also on other factors, such as the depth of the upper mixed layer and the attenuation coefficient in the water column, among others. The light in both chambers was provided by 10 cool-white fluorescent lamps (Philips daylight, 1.2 m long, 40 W), and photon flux density was measured with a spherical micro quantum sensor (Walz GmbH, model US-SQS/WB). During the acclimation period, the cultures were diluted every other day to keep the cells in the exponential growth phase (Chl *a* between 15 and 40 μg L^{-1}). The growth rates (μ) of *T. weissflogii* at 20°C and 25°C were 0.63 d^{-1} (standard deviation [SD] = 0.04) and 0.8 d^{-1} (SD = 0.05), respectively. After the acclimation period, the cultures were transferred to UVR-transparent polycarbonate (XT tubes, Rohm and Haas) or to quartz vessels and were exposed outdoors, as described below. The experiments were done in late spring 2008 (24–28 November) at the EFPU (43°18′42.38″S, 65°02′30.42″W) in Patagonia, Argentina.

Experimentation and radiation treatments—Two types of experiments were carried out: full day–length exposures and short-term (i.e., 1-h) exposures. The daily cycle experiments were carried out on 24 November, while the short-term exposures were done on 25 November (day of the year [DOY] 329). The results obtained from the three daylight experiments were similar, so in this article we are only presenting the data derived from the daily cycle experiment done on 24 November (DOY 238) and from the short-term experiment performed on 25 November (DOY 239), as during these two days we had a complete data set (i.e., more variables were measured).

Daily cycles: Cultures of *T. weissflogii* were diluted to cell densities measuring between 8×10^3 cells mL^{-1} and 4×10^4 cells mL^{-1} just prior to the outdoor exposure and were transferred to various vessels, as follows: (1) 800-mL UVR-transparent polycarbonate for Rubisco measurements; (2) 500-mL quartz tubes for pigment analysis; (3) 50-mL quartz tubes for Chl *a* fluorescence measurements, and (4) 20-mL quartz tubes for carbon incorporation. For all measurements (with the exception of Rubisco, due to volume constraints), three radiation treatments were implemented: (1) full solar radiation—PAB treatment: PAR + UV-A + UV-B (280–700 nm)—uncovered vessels; (2) PA treatment: PAR + UV-A (320–700 nm)—vessels covered with UV cut-off filter foil (Montagefolie, No. 10155099, Folex); and (3) P treatment: only PAR (400–700 nm)—vessels covered with Ultraphan film (UV Opak, Digefra). For Rubisco measurements only

the PAB and P treatments were done. The transmission spectra of these filters and materials are published elsewhere (Figueroa et al. 1997; Villafañe et al. 2003).

The vessels were placed in an outdoor thermostatic water bath (Frío 21) equipped with two independent temperature circuits. The experimental temperatures were set to 20°C and 25°C (± 1°C). Exposure started at 08:00 h and ended at 17:00 h. Every 60–90 min samples were withdrawn from the water baths, as further described below.

Short-term exposures: These 1-h incubations were centered on local noon, with treatments as explained above for daily cycles. The outdoor exposures started at ca. 11:30 h and 13:30 h, and every 10–15 min samples were withdrawn, transported to the laboratory under dim light, and immediately processed, as further described below. Two short-term exposures were done during the study period, and radiation treatments were PAB and P only.

Sampling protocol, analysis, and measurements—Solar radiation: Incident solar radiation over the study area was monitored continuously using a broadband European Light Dosimeter Network (ELDONET) radiometer (Real Time Computers) permanently installed on the roof of the EFPU. The instrument measures UV-B (280–315 nm), UV-A (315–400 nm), and PAR (400–700 nm) with a frequency of one reading per second and stores the minute-averaged values for each channel.

Carbon incorporation: A total of 36 quartz tubes (20 mL) per temperature level were placed in the water bath at the start of both short-term and daily cycle experiments, with 12 tubes subjected to PAB, 12 tubes to PA, and 12 tubes to the P treatments. Each tube was inoculated with 0.1 mL containing 5 μCi (0.185 MBq) of ^{14}C-labeled sodium bicarbonate (ICN Radiochemicals). After every 90 min (daily cycles) or 15 min (short term) of exposure, triplicates tubes from each radiation treatment were withdrawn and filtered immediately onto a Whatman GF/F filter (25-mm diameter). The filters were then placed in 7-mL scintillation vials, exposed to HCl fumes overnight, and dried. After this step, scintillation cocktail (HiSafe' 3, Perkin Elmer) was added, and the samples were counted using a liquid scintillation counter (Holm-Hansen and Helbling 1995).

Chl *a* fluorescence parameters: A total of six quartz tubes per temperature level were exposed to solar radiation under the three radiation treatments, giving duplicates per treatment. Samples (5 mL) were taken every ca. 90 min (daily cycles) or 10 min (short term), and in vivo Chl *a* fluorescence parameters of the PSII were determined using a portable PAM fluorometer (Walz, model Water-ED PAM). At noon (only during the daily cycles) and at the end of the exposure period (in both daily cycles and short-term exposures) subsamples from each tube were placed inside the growth chambers (at 20°C and 25°C), and the recovery of fluorescence parameters in dim light (< 10 μmol quanta m^{-2} s^{-1}) was followed for 12 h, measuring each sample every ca. 30 min (in daily cycles) or 10 min (in short-term exposures). Each sample was measured six times immediately after sampling, without any dark adaptation. The effective photochemical quantum yield (Y) was calculated using the equations of Genty et al. (1989) and Weis and Berry (1987), as follows:

$$Y = \Delta F : F'_m = (F'_m - F_t)/F'_m \quad (1)$$

where F'_m is the maximum fluorescence induced by a saturating light pulse (ca. 5300 μmol quanta m^{-2} s^{-1} in 0.8 s) and F_t is the current steady-state fluorescence induced by a weak actinic light (82 W m^{-2}) in light-adapted cells. The NPQ of Chl *a* fluorescence was determined by measuring F_m at the start of the experiments in samples maintained in darkness and F'_m during the exposure time, as follows:

$$NPQ = (F_m - F'_m)/F'_m \quad (2)$$

There were no significant differences between NPQ values calculated in this way and those obtained directly using the PAM fluorometer. As a result, we used the values obtained directly with the instrument.

Pigment analysis: Every 90 min, duplicate 50-mL aliquots were obtained for pigment analysis (in daily cycle experiments only). Samples were immediately filtered on GF/F filters (Whatman, 25-mm diameter) by mild vacuum (< 10 mm Hg) and were then frozen and stored in liquid nitrogen. After transportation to The Netherlands in liquid nitrogen, the samples were freeze-dried and pigments were extracted in 90% acetone overnight in darkness at 4°C. Pigments were resolved by high-performance liquid chromatography (HPLC; Waters) with a C18 5-μm Delta Pack reversed-phase column (Milford) following the technique described in Van Leeuwe et al. (2006). Pigment identification was done by retention time and diode array spectroscopy (Waters). Chl *a*, fucoxanthin, diadinoxanthin (DD), and diatoxanthin (Dt) standards (DHI) were used for quantification. Cellular pigment concentrations were calculated from cell counts and extraction volume.

Chl *a* concentration was measured twice, once for pigment fingerprinting (using HPLC, as described above) and once for calculations of carbon assimilation numbers, using fluorometry and spectrophotometry. HPLC-derived Chl *a* concentration and fluorometer-derived Chl *a* data were highly correlated. At the beginning of each experiment aliquots of 50–100 mL of sample were filtered onto Whatman GF/F filters (25-mm diameter); the filters were then placed in centrifuge tubes (15 mL) with 5 mL of absolute methanol (Holm-Hansen and Riemann 1978). The tubes containing the methanolic extract and filters were placed in a sonicator for 20 min (20°C or 25°C, according to the experiment) and then in the dark (4°C) for at least 1 h. After the extraction period the sample was centrifuged (15 min at 1750 × *g*) and scanned (250–750 nm) in a Hewlett Packard diode-array spectrophotometer (model HP 8453 E) using a 5-cm–path length cuvette; Chl *a* concentration was calculated using the equation of Porra (2002). The same sample was used to calculate Chl *a* concentration from the fluorescence of the extract (Holm-Hansen et al. 1965) before and after acidification (1 mol L^{-1} HCl) using a fluorometer (Turner Designs, model TD 700).

The fluorometer was calibrated using purified Chl *a* from *Anacystis nidulans* (Sigma No. C 6144).

Rubisco activity: For each radiation condition, triplicate samples (100 mL) were filtered onto 2.0-μm pore-size polycarbonate filters (Osmonics), immediately frozen in liquid nitrogen, and stored at -80°C until further analysis. Rubisco activity was determined following the procedure of Gerard and Driscoll (1996). Crude enzyme extracts were prepared by transferring the filters to test tubes containing ice-cold extraction buffer (25 mmol $KHCO_3$, 20 mmol $MgCl_2$, 0.2 mmol ethylenediamine tetraacetic acid [EDTA], 5 mmol dithiothreitol [DTT], 0.1% Triton X100, and 50 mmol 4-(2-hydroxyethyl)-1-piperazineethanesulfonic acid [HEPES]-KOH, pH 8.0). The cells were disrupted by sonication, after which the extracts were centrifuged for 15 min (20,000 $\times$ *g*) at 4°C. Fifty microliters of supernatant was used for protein determination (BioRad Protein Assay), and 150 μL was used for the Rubisco activity assay. The Rubisco assay mixture (pH 8.0) contained 25 mmol $KHCO_3$, 20 mmol $MgCl_2$, 0.2 mmol EDTA, 5 mmol DTT, 50 mmol HEPES-KOH, 3 mmol adenosine 5′-triphosphate, 0.2 mmol nicotinamide adenine dinucleotide (NADH), 5 mmol phosphocreatine, 22 units of creatine phosphokinase, 9 units of glyceraldehyde-3-phosphate dehydrogenase, and 18 units of 3-phosphoglyceric phosphokinase.

The mixture was placed in a Cary 3E UV : Vis spectrophotometer, and after temperature equilibration to 20°C the background oxidation of NADH (absorbance at 340 nm) was followed for several minutes. The reaction was started by adding 2 mmol (final concentration) ribulose-1,5-bisphosphate, and the time course of NADH oxidation was recorded by the decrease in absorbance at 340 nm. The background oxidation of NADH was subtracted from the measured activity, which was expressed as the declining absorbance per milligram of total protein per second (mAbs340 mg protein^{-1} s^{-1}).

Rubisco gene expression: For each radiation condition, triplicate samples (100 mL) were filtered over 2.0-μm pore-size polycarbonate filters (Osmonics), immediately frozen in liquid nitrogen, and stored at -80°C until later analysis. Rubisco gene expression was determined by quantitative real-time polymerase chain reaction (RT-PCR) of the large subunit of Rubisco. RNA was isolated using TRIzol^{R} Reagent (1 mL per sample), according to the manufacturer (Invitrogen Life Technologies). The isolated RNA was subsequently treated with DNase I (Amersham Bioscience). RNA concentrations and purity were determined on a Nanodrop ND-1000 spectrophotometer (NanoDrop Technologies). First strand complementary DNA (cDNA) was synthesized from 65 ng of DNA-free RNA using 500 ng oligo (dT) 12, 18 primer, and Superscript III H reverse transcriptase (Invitrogen Life Technologies). cDNA concentrations were also determined on the Nanodrop ND-1000 spectrophotometer. Based on an alignment of known algal Rubisco large subunit sequences, primers for *T. weissflogii* were designed using the program Primer3 (Rozen and Skaletsky 2000). The designed Rubisco forward (5′-AAAATGGGTTACTGGGATGCTTC-3′) and Rubisco reverse (5′-CAGCAGCTTCTACTGGATCTACACC-3′) primers were synthesized by Biolegio B.V. (Nijmegen). Amplification with these primers resulted in the expected 102–base pair fragment for *T. weissflogii*. Quantitative RT-PCR (qRT-PCR) was performed using an iCycler 1 (BioRad).

cDNA amplification reactions were performed in triplicate for every sample in a final reaction mixture of 15 μL, containing 1 μL cDNA (10 ng μL^{-1}), 7.5 μL Power SYBR Green Master Mix (Applied Biosystems), 0.5 μL of both forward and reverse primer (20 μmol), and 5.5 μL H_2O. The amplification reaction was executed as follows: 2 min at 50°C and 10 min at 95°C, followed by 40 cycles of 15 s at 95°C and 60 s at 60°C. Melting curves for excluding nonspecific PCR side products were acquired by heating the products for 15 s at 95°C and 1 min at 55°C, subsequent quick heating to 60°C, followed by a more steady heating to 95°C with increments of 0.5°C : 10 s^{-1}. PCR amplifications without template (solely H_2O) and RNA samples without treatment with reverse transcriptase were used as controls. Four cDNA dilutions (1, 10, 100, and 1000 ng) were used to estimate the efficiency in a validation experiment. Individual PCR efficiency was calculated (Ramakers et al. 2003) to bypass the assumption that in all samples the PCR efficiency is constant. The triplicate PCR reactions per sample were averaged before performing the $2^{-\Delta\Delta C_T}$ method (Livak and Schmittgen 2001). Relative quantification was presented as the fold in change in mRNA transcript level relative to the sample with the lowest number of mRNA transcripts present.

Data treatment—The data are reported either as mean and half mean range (when duplicate samples or measurements were done) or as mean and SD when more replicates were obtained. The inhibition by UV-B, UV-A, and UVR, respectively, was calculated as follows:

$$UVB_{inh}(\%) = 100(P_{PA} - P_{PAB}) : P_P \quad (3)$$

$$UVA_{inh}(\%) = 100[(P_P - P_{PA})] : P_P \quad (4)$$

$$UVR_{inh}(\%) = 100[(P_P - P_{PAB})] : P_P \quad (5)$$

where P_P, P_{PA}, and P_{PAB} represent either the carbon fixation or the effective photochemical quantum yield of samples in the P, PA, and PAB treatments, respectively.

A one-way repeated-measurements ANOVA test was used to determine differences among radiation treatments and temperatures. A two-way ANOVA test was used to determine interactions between factors (i.e., irradiance and temperature), both using a 95% confidence limit (Zar 1999). When the data did not follow homoscedasticity, the non-parametric Kruskal–Wallis test was used to assess significant differences between the samples.

Results

Solar radiation was variable during the experimental period, with a maximum PAR level (Fig. 1A) of almost 500 W m^{-2}, while UV-A (Fig. 1B) and UV-B (Fig. 1C) reached maximum values of 70 W m^{-2} and 2 W m^{-2}, respectively. Most of the day-to-day variability was due to variations in

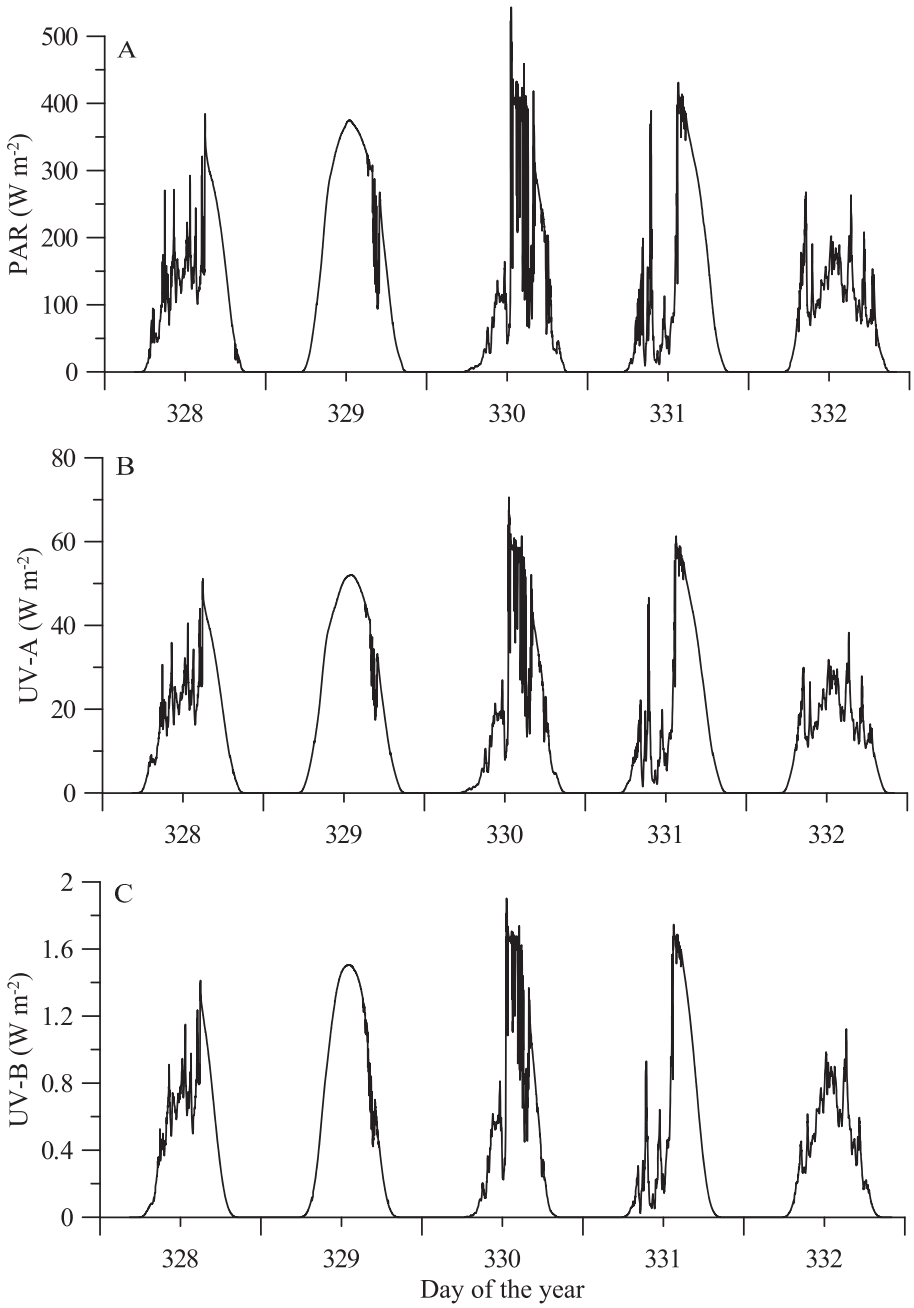

Fig. 1. Irradiance levels (in W m^{-2}) during the experimental period (24–28 November 2008; DOY 328 to 332) for (A) PAR (400–700 nm), (B) UV-A (315–400 nm), and (C) UV-B (280–315 nm).

cloud cover, ranging from an almost completely covered day (DOY 332) to an almost cloudless day (DOY 329).

The daily course of carbon incorporation measured during a cloudy day (DOY 328) showed significant differences ($p < 0.05$) between radiation treatments at 20°C toward the end of the incubation (Fig. 2A). A much higher rate of carbon incorporation was attained at 25°C, and no significant inhibition was observed among radiation treatments at this temperature (Fig. 2B). During the short-term incubations (Fig. 2C,D), which were done during a clear day (DOY 329, *see* Fig. 1), the cultures of *T. weissflogii* were much more inhibited than during the previous day (DOY 328): Carbon fixation of samples incubated at 20°C was immediately inhibited after exposure, and the differences between the PAB and P treatments significantly increased as the incubation progressed (Fig. 2C). At 25°C (Fig. 2D)—and despite the fact that UVR inhibition was significant ($p < 0.05$)—the differences were smaller than those observed at 20°C; again, a higher rate of carbon incorporation was attained at the high temperature.

The differences between exposures at both temperatures were further evident when considering the assimilation numbers at the end of the incubation period (Fig. 3): The assimilation numbers at 25°C were significantly higher ($p <$

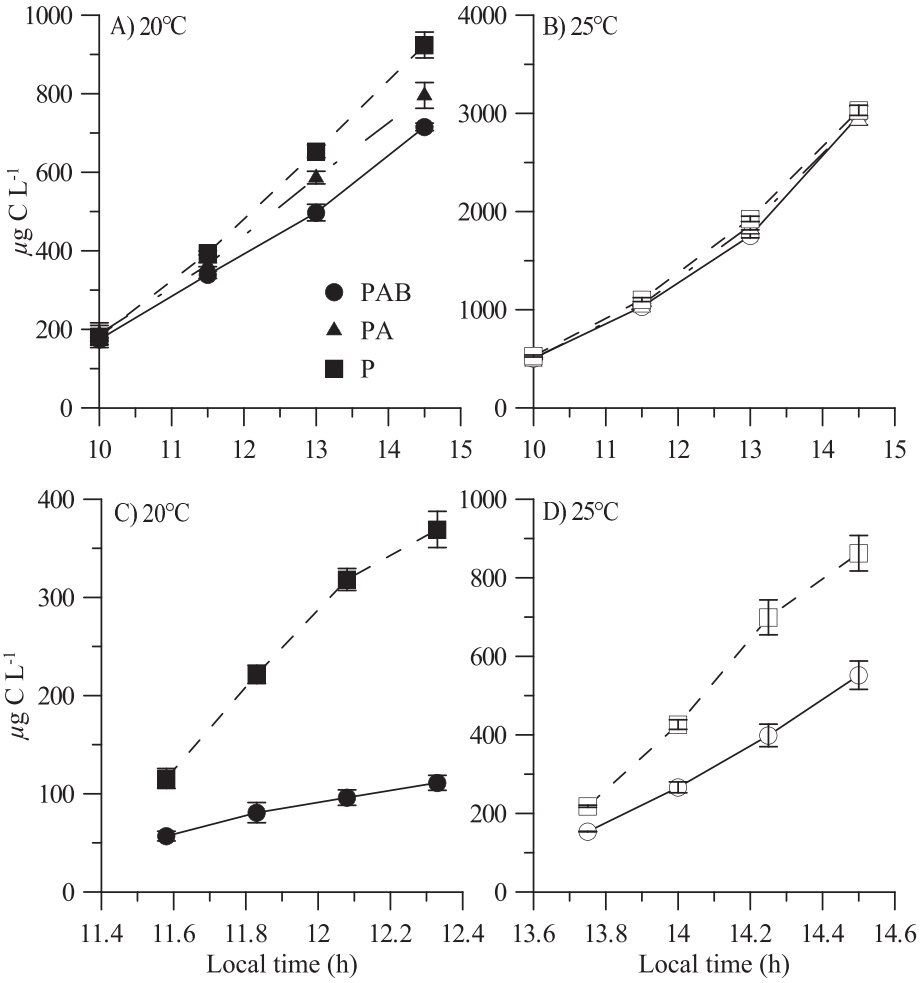

Fig. 2. Carbon fixation (in μg C L^{-1}) of *Thalassiosira weissflogii* during experiments carried out during spring 2008 in Patagonia. Results of daily cycle (DOY 328) are expressed as (A) carbon fixation of samples incubated at 20°C and (B) carbon fixation of samples incubated at 25°C. Representative results of a short-term incubation (DOY 329) are expressed as (C) carbon fixation of samples incubated at 20°C and (D) carbon fixation of samples incubated at 25°C. The symbols represent the mean of triplicate samples under the different radiation treatments, while the vertical lines are the SD. Solid symbols indicate samples exposed at 20°C, whereas open symbols indicate samples exposed at 25°C.

0.05) than those at 20°C for all radiation treatments and for both types of incubations. During the daily cycle (Fig. 3A), carbon fixation in the PAB treatment at 20°C was significantly reduced ($p < 0.05$) by UVR (i.e., 22%, as compared to the P treatment), with UV-B and UV-A accounting for 38% and 62%, respectively, of total inhibition. Based on assimilation numbers, the inhibition due to UVR at the end of the short-term incubations (Fig. 3B) was 70% and 36% for cultures at 20°C and 25°C, respectively.

Effective photochemical quantum yield (Y) of *T. weissflogii* samples measured during the daily cycle (Fig. 4A,C,E) and short-term exposures (Fig. 4B,D,F) showed significant differences ($p < 0.05$) between radiation treatments as well as between incubation temperatures. During the daily cycle, and at all times during exposure (mean UVR of 26.1 ± 8.9 W m^{-2}), samples incubated at 20°C (Fig. 4A) under UVR (i.e., PAB and PA treatments) showed a significantly lower Y compared to those in the P treatment. Recovery of Y was not evident during the exposure period (i.e., during the afternoon), but it did occur when samples were transferred to dim light, either at noon or at the end of the exposure period. When *T. weissflogii* samples were incubated at 20°C during short-term exposures, but at higher irradiances (mean UVR of 52.3 ± 1.1 W m^{-2}, Fig. 4B), the observed inhibition of Y was significantly higher, and recovery was not complete even after 1 h under dim light. At 25°C and during both daily and short-term exposures (Fig. 4C,D), Y values were significantly higher than those at 20°C. The recovery of samples during the daily cycle was complete when the samples were transferred to dim light (Fig. 4C); however, during the short-term exposure the recovery was not complete, with Y values at the end being significantly lower than at the beginning of incubation (Fig. 4D). The calculated UVR inhibition of Y for both the daily cycle (Fig. 4E) and the short-term exposures (Fig. 4F) showed

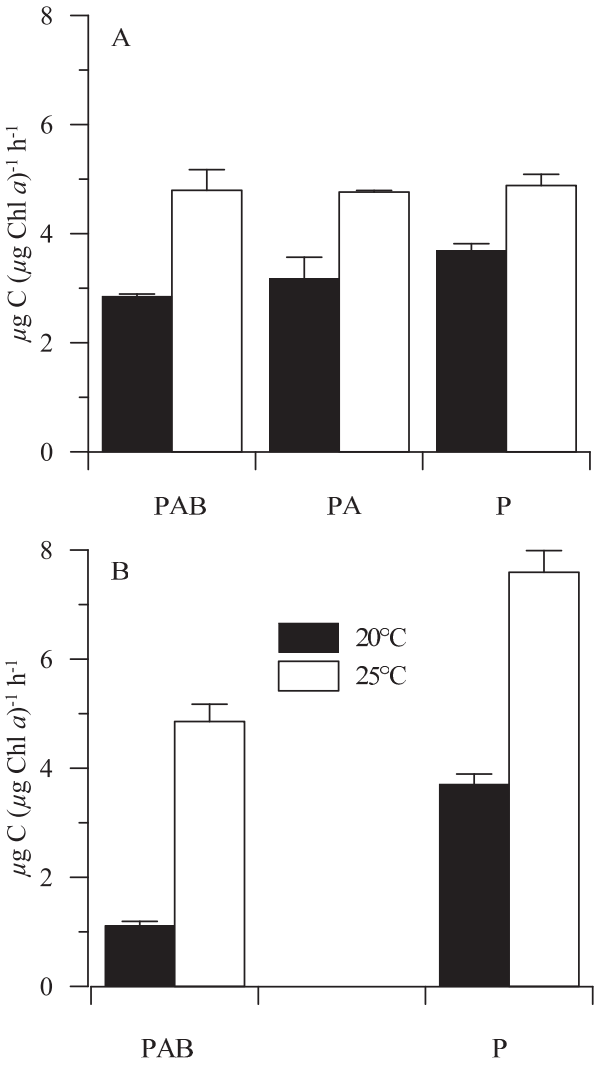

Fig. 3. Assimilation numbers (in μg C [μg Chl a]$^{-1}$ h^{-1}) of *Thalassiosira weissflogii* at the end of the incubation period for samples incubated at 20°C and 25°C. (A) Daily cycle (DOY 328); (B) short-term incubation (DOY 329). The bars represent the mean of triplicate samples under the different radiation treatments, while the vertical lines are the SD. Black bars indicate samples exposed at 20°C, whereas open bars indicate samples exposed at 25°C.

significantly lower values in samples incubated at 25°C compared to those incubated at 20°C. The mean UVR inhibitions during the daily cycle were 11.9% ± 6.9% and 41.7% ± 6.6% for incubations at 25°C and 20°C, respectively. During the short-term incubations (Fig. 4F), the mean UVR inhibition decreased from a value of 72.4% ± 8.9% at 20°C to a value of 39.6% ± 5.7% at 25°C.

Photoprotective activity of *T. weissflogii* during the daily cycle was assessed through the evaluation of the de-epoxidation state (DEPS: Dt : (Dt + DD), as well as from heat dissipation mechanisms (i.e., NPQ) (Fig. 5C). The initial DEPS was low early in the morning, but it increased significantly when samples were exposed to solar radiation (Fig. 5A). By noon, samples incubated at 20°C had a higher DEPS than those incubated at 25°C, and these differences among the same radiation treatment but at different temperatures were maintained throughout the exposure. There were no significant differences in DEPS among radiation treatments at 20°C, but DEPS in samples under the PAB at 25°C were significantly higher than those in the P treatment (Fig. 5A).

Photoprotective capacity, expressed as the ratio of xanthophyll to photosynthetic pigments, was significantly higher at 25°C than at 20°C (Fig. 5B) before and during the outdoor exposures (Table 1). At both temperatures, the ratio changed during the outdoor exposures, in favor of the xanthophyll pigment pool. However, as was the case with the DEPS responses, there were no differences among radiation treatments. Finally, heat dissipation mechanisms via NPQ were much more evident at 20°C than at 25°C (Fig. 5C). Moreover, at 20°C NPQ increased as the experiment progressed, with samples under the PAB treatment having the highest NPQ, followed by those under the PA treatment (Fig. 5C).

During the daily cycle, Rubisco activity and gene expression were significantly affected by temperature (Fig. 6). In general, Rubisco activity was relatively constant during the daily cycle, but cultures incubated at 25°C showed significantly higher activity compared to those incubated at 20°C (Fig. 6A). However, there were no significant differences among radiation treatments. Rubisco gene expression was significantly higher in samples incubated at 25°C compared to those incubated at 20°C (Fig. 6B). At 20°C, Rubisco gene expression was rather similar throughout the exposure; however, at 25°C, gene expression showed an optimum around noon.

Discussion

Photosynthesis is a complex process that depends on the action of a large number of enzymes, as well as on the availability of substrates (i.e., CO_2 and H_2O). Therefore, it is highly probable that a particular stressor will affect one or more targets simultaneously. The picture is further complicated when considering a multi-factor experimental approach, with the combined effect either being synergistic or antagonistic (Dunne 2010). Climate change resulting from anthropogenic activities (IPCC 2007) simultaneously modifies several variables that in turn affect photosynthesis. One such stressor of photosynthesis is UVR, which is known to reduce photosynthetic rates of phytoplankton organisms (*see* reviews by Villafañe et al. [2003] and Harrison and Smith [2009]). Another interfering factor is the temperature increase, and the evaluation of its effects deserves special interest not only in the aquatic environment but with regard to the Earth as a whole (IPCC 2007). Recent reports (Mckenzie et al. 2011) indicate that solar UV-B radiation reaching the Earth's surface might not increase further in the future and that the ozone layer might start to recover. Nevertheless, aquatic organisms such as phytoplankton would experience an increase in solar radiation as a feedback mechanism due to climate change: Increased water temperature (due to climate change) would produce a shallower thermocline and thus reduce the depth of the upper mixed layer, thus exposing phytoplankton to higher radiation conditions as well as to higher temperatures.

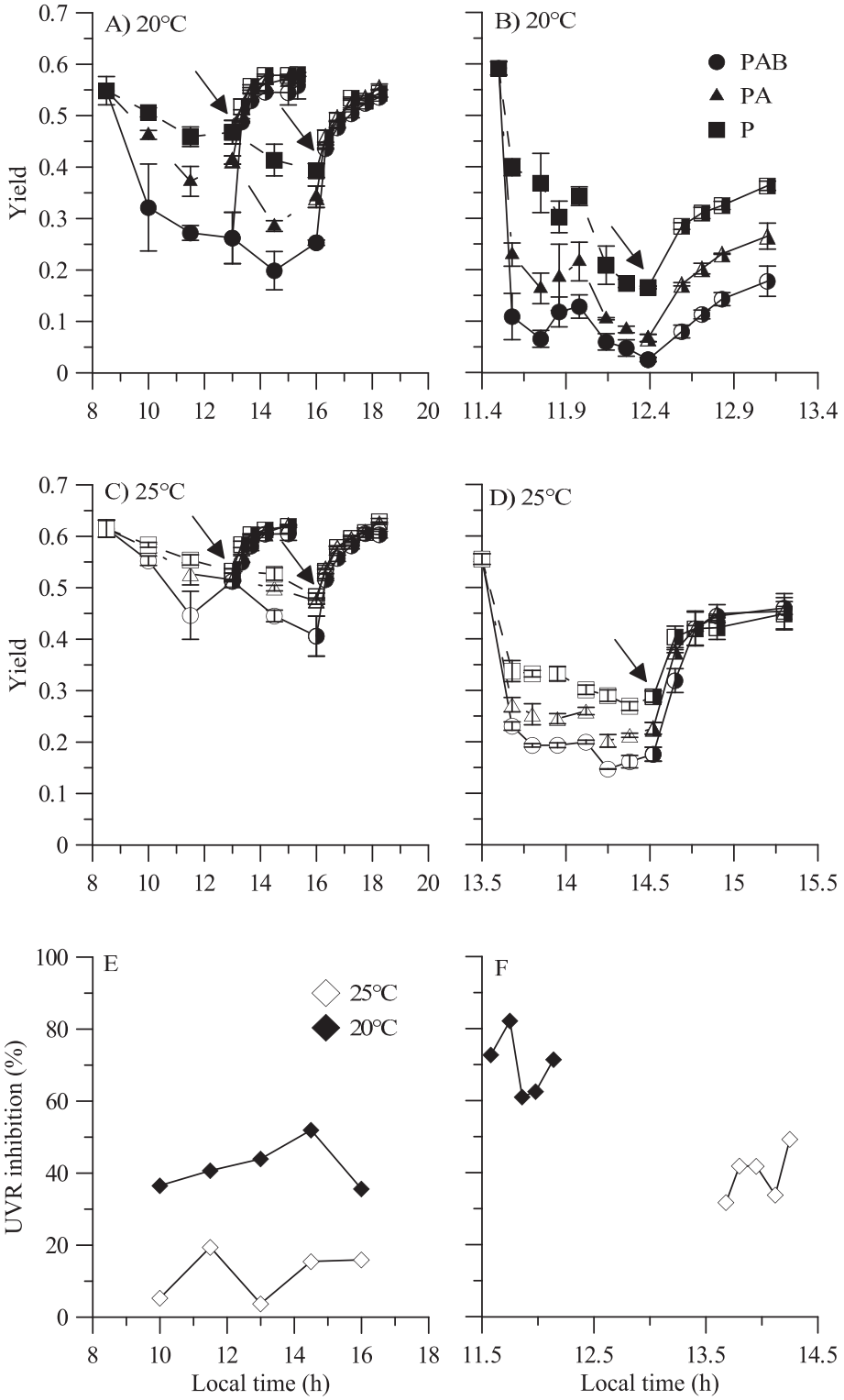

Fig. 4. Effective photochemical quantum yield of *Thalassiosira weissflogii* samples exposed to solar radiation under the three radiation treatments (PAB, PA, and P) during (A) daily cycle (DOY 328) at 20°C; (B) representative short-term exposure at 20°C (DOY 329); (C) daily cycle at 25°C; (D) representative short-term exposures at 25°C. UVR-induced inhibition of Y at 20°C and 25°C during (E) daily cycles and (F) short-term exposure. Circles, triangles, and squares represent the mean of duplicate samples, while the vertical lines are the half-mean range. Solid symbols indicate samples exposed at 20°C, whereas open symbols indicate samples exposed at 25°C. Half-filled symbols after the arrows indicate recovery in dim light in the laboratory.

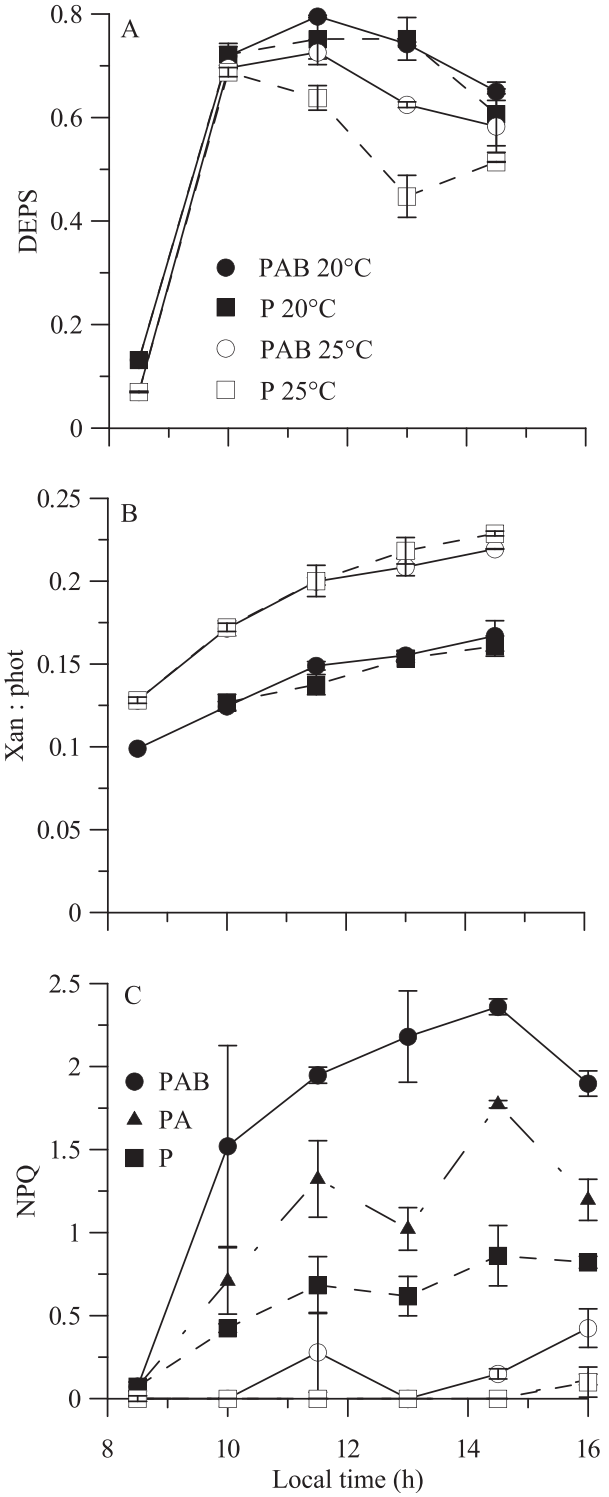

Fig. 5. Xanthophyll pigments in *Thalassiosira weissflogii* under different radiation treatments (circles: PAB; squares: P) and temperatures (solid symbols: 20°C; open symbols: 25°C) throughout the daily cycle (DOY 328). (A) DEPS, calculated as Dt : (Dt + DD); (B) ratio of xanthophyll to photosynthetic (xan : phot) pigments; (C) NPQ. The symbols represent the mean of duplicate samples, while the vertical lines are the half-mean range.

While most investigations dealing with the effects of UVR on phytoplankton photosynthesis have evaluated carbon fixation occurring during the 'dark' reactions (Calvin–Benson cycle: i.e., through radiocarbon incorporation measurements), some others have focused on more specific targets, such as Rubisco (Lesser 1996*a*; Bouchard et al. 2008), xanthophyll pigments (Van De Poll and Buma 2009), carbonic anhydrase activity (Wu and Gao 2009), and the electron transport rate of PSII (Bergmann et al. 2002; Villafañe et al. 2007; Bouchard et al. 2008). On the other hand, increased temperatures have been known to affect phenology and biodiversity (Wrona et al. 2006) as well as plant–herbivore dynamics and food-web length (Beisner et al. 1997), among many other effects. Still, and at the individual level, increased temperatures seem to directly and indirectly favor different physiological processes in aquatic organisms (Sobrino and Neale 2007; Halac et al. 2010; Hernández Moresino and Helbling 2010).

Previous studies addressing the interactive effect of temperature and UVR on *T. pseudonana* concluded that temperature affected the sensitivity to UVR mainly because of changes in the rates of repair for similar rates of damage (Sobrino and Neale 2007). The study of Halac et al. (2010) obtained a similar conclusion for *Chaetoceros gracilis*, but even though an increase in temperature resulted in a better photosynthetic response of *T. weissflogii*, the underlying physiological mechanisms were not clear, and the authors speculated that the differences in responses between the two species were probably related to their size or to their distribution within the oceanic realm (i.e., coastal vs. oceanic).

In this work we thoroughly evaluated the photosynthetic responses of the cosmopolitan diatom *T. weissflogii* when exposed to different radiation and temperature treatments, targeting both the photosystem and the Calvin–Benson cycle levels. Our data show a degree of responses in relation to the exposure to different radiation treatments (i.e., ranging from the characteristic inhibitory response [e.g., Figs. 2–4] to no significant effects [e.g., Fig. 5]). These differences with regard to UVR exposure were observed not only when comparing different time scales of experimentation (i.e., short-term exposures vs. daily cycles) but also different stages of the photosynthesis process, which vary within a range of seconds (or fractions) to hours (Falkowski 1984; Laney 2006). Additionally, differences in responses were affected by incubation temperature, with higher values generally benefiting the species, by reducing UVR-induced photoinhibition on PSII (Fig. 4) as well as in the Calvin–Benson cycle (Figs. 2, 3). In addition, and although the xanthophyll cycle pigments (per cell) were not different between the two temperatures (Table 1), there was a higher protective capacity at the higher temperature due to a higher xanthophyll : photosynthetic pigment ratio (Fig. 5). This difference was mainly due to a lower content of Chl *a* per cell at higher temperatures (Table 1). The growth rate (*see* above) was significantly higher at 25°C than at 20°C, indicating that as a result of the faster growth, cells growing at 25°C were slightly smaller and thus had a smaller amount of Chl *a* per cell. Finally, there was a significant increase in Rubisco activity and gene expression at the higher temperature (Fig. 6). All of these data clearly

Table 1. Chlorophyll and xanthophyll concentration per cell (pg cell^{-1}) in the three radiation treatments (PAB, PA, and P) at 20°C and 25°C at various times during the daily cycle experiment.

Concentration (pg cell^{-1}) and time (h)	20°C			25°C		
	PAB	PA	P	PAB	PA	P
Chlorophyll						
0	5.34	5.34	5.34	4.33	4.33	4.33
1.5	4.41±0.38	5.20±0.13	4.64±0.25	3.70±0.36	3.93±0.13	3.80±0.13
6	4.79±0.29	4.40	4.72±0.38	3.23±0.09	3.26±0.17	3.19±0.31
Xanthophyll						
0	0.69	0.69	0.69	0.74	0.74	0.75
1.5	0.71±0.04	0.81±0.03	0.77	0.83±0.06	0.89±0.05	0.85±0.02
6	1.02±0.12	0.94	0.97±0.11	0.91±0.03	0.93±0.09	0.95±0.08

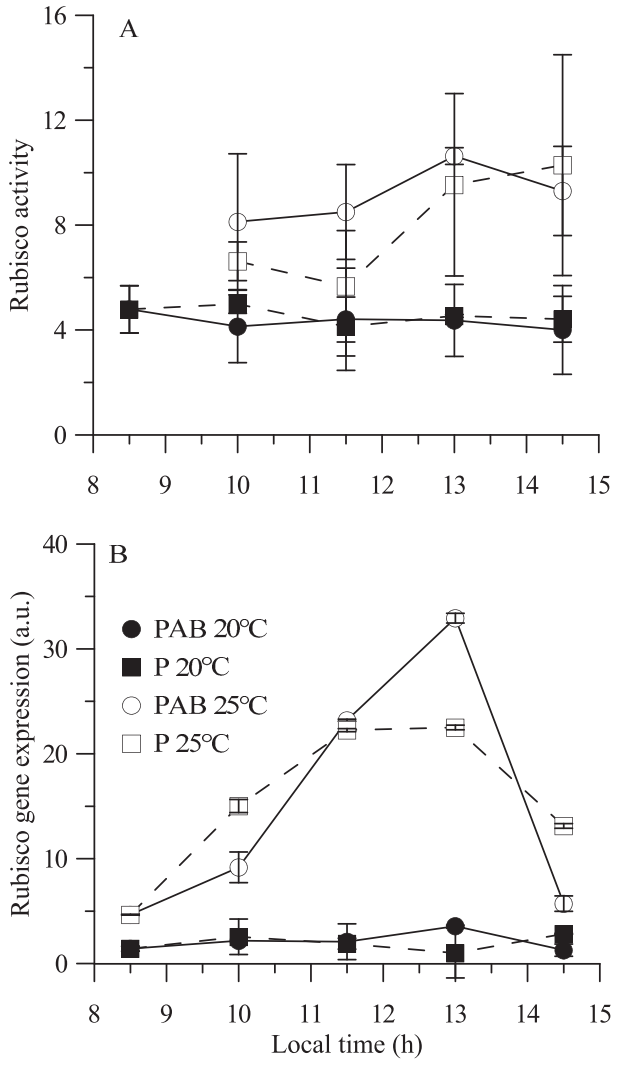

Fig. 6. (A) Rubisco activity (mAbs340 mg protein^{-1} s^{-1}) and (B) relative Rubisco gene expression (arbitrary units [a.u.]) during the daily cycle (DOY 328) at different radiation treatments (circles: PAB; squares: P) and temperatures (solid symbols: 20°C; open symbols: 25°C). The symbols represent the mean of duplicate samples, while the vertical lines are the half-mean range.

point out that the physiological 'strategy' of *T. weissflogii* involves multiple adjustments that are related to different targets, as discussed below.

The samples exposed to solar radiation at 20°C had a significant effect related to UVR reduction of carbon fixation, which was noticeable in both the daily cycle and the short-term incubations (Figs. 2, 3). There was a characteristic response when cells were exposed to different wave bands, with UV-A accounting for the bulk of inhibition, as seen in many environments of the world (Villafañe et al. 2003). During our study, however, larger differences among radiation treatments of samples incubated at 20°C were observed during the short-term incubation, which could be related mainly to the higher radiation levels on DOY 329 (Fig. 1). Similarly, higher inhibition due to UVR at both temperatures was observed for Y during short-term incubations (Fig. 4F), as compared to the daily cycle (Fig. 4E). Still, there was a clear trend of recovery of Y, which was complete in the daily cycle, as compared to the short-term incubation. However, the magnitude of UVR-induced effects (as well as those due to PAR) on carbon fixation and PSII fluorescence was clearly reduced by exposure at the higher temperature (Figs. 3, 4), but this beneficial effect of temperature does not seem to be universal, as there is a significant species-specificity component. For example, high temperatures might lead to enhanced superoxide radical production, as observed for symbiotic dinoflagellates (Lesser 1996*b*). Furthermore, the study of Halac et al. (2010) found that although high temperature (23°C, i.e., either during acclimation or exposure) generally benefited photosynthetic performance of *T. weissflogii* and *C. gracilis*, the latter seemed to adjust better to the change from 18°C to 23°C. This was probably related to a more efficient mechanism of energy dissipation, such as NPQ, which was less evident in *T. weissflogii*. In contrast to this finding, in our study the energy dissipation (evaluated via DEPS, calculated as Dt/[Dt + DD]) was higher at the lower temperature (Fig. 5A). On the other hand, the xanthophyll pigment pool relative to photosynthetic pigments was higher at 25°C throughout the outdoor exposure period (Fig. 5B), and, therefore, less conversion to Dt might be required to give the same level of heat

dissipation (Van De Poll and Buma 2009). Xanthophyll pigments are thought to have a photoprotective function against UVR stress in some species, and sometimes a higher de-epoxidation state is associated with exposure to these wavelengths (Van De Poll et al. 2010), as was also seen in our study (Fig. 5A). However, possibly enhanced de-epoxidation might be a result of damage that has already occurred rather than a result of effectively functioning in the prevention of damage (Buma et al. 2009).

Finally, both Rubisco activity and gene expression throughout the daily cycle (Fig. 6) had higher levels at higher temperatures, thus hinting for a positive feedback of temperature on photosynthesis. The higher Rubisco activity and gene expression at 25°C indicate that more photons can be processed and, thus, less dissipation of excess energy as heat might be needed. In fact, this was observed in our data, as *T. weissflogii* had higher effective photochemical quantum yield (Fig. 4) and less energy dissipation (NPQ, Fig. 5) at 25°C, as compared to samples at 20°C. In addition, this overall process was tightly coupled with the higher assimilation number at 25°C (Fig. 3) and significantly less photosynthetic inhibition due to UVR at this high temperature (Figs. 2–4). These increases in Rubisco activity and gene expression, as demonstrated in our study, clearly indicate a different cell strategy compared to the ones previously documented (Sobrino and Neale 2007; Halac et al. 2010). The differences in mechanism (i.e., increased repair rates [Sobrino and Neale 2007] or higher dissipation of energy [Halac et al. 2010] vs. increases in Rubisco activity and gene expression) have different consequences for aquatic biota. While an increase in Rubisco activity would mean more carbon fixed and, thus, higher production, the use of energy to accomplish the repair or the dissipation of excess energy, comparatively, would mean less production.

In aquatic ecosystems, direct and indirect effects of increased temperature can be observed. In the case of mid-latitudes, as characterized our study site, phytoplankton experience great changes throughout the year, not only in terms of temperature and the depth of the upper mixed layer but also in terms of solar radiation impinging the sea surface (Villafañe et al. 2004). The lowest temperature used in our experiments (20°C) is close to the mean summer seawater surface value of 18°C along the Patagonian coast and is within the observed range of temperatures during summer (Villafañe et al. 2004; Helbling et al. 2010). However, we imposed an increase of 5°C over the in situ value, as was predicted for the year 2100 (Houghton et al. 2001). During summer, *Thalassiosira* species are the most abundant species in the plankton in Patagonian waters, accounting for over 50% of the total phytoplankton species abundance (Villafañe et al. 2008). If the mechanism that we propose for coping with UVR and temperature stress (i.e., increases in Rubisco activity and gene expression) is rather general for *Thalassiosira*, as a result of their abundance, a potential temperature increase during summer would increase the productivity of the area during this season, with a potential increase in the already-high secondary production in the area (Skewgar et al. 2007). On the other hand, it might be expected that the effect of increased temperature on UVR effects in the water column might be different during winter, as a result not only of the normal low temperatures and solar radiation levels but also of the different phytoplankton species composition, with blooming microplankton *Odontella aurita* (Villafañe et al. 2004). Nevertheless, it has to be considered that in nature, changes in water column temperature would also lead to changes in increased stratification, which, in turn, would modify not only the exposure of cells to solar radiation but also the availability of nutrients within the upper mixed layer (Beardall et al. 2009). Overall, the net response of natural phytoplankton to climate change variables will not lie in the specific effect of each variable but rather in their combined effects. Additionally, and based on this study as well as others, it seems to be a significant component of species specificity in the observed responses.

Acknowledgments

We thank R. Villanueva, M. Lagunas, and E. Heimsch for their help during experiments, and we thank H. Zagarese for the radiocarbon measurements. We also appreciate the comments and suggestions of three anonymous reviewers and of the Associate Editor of *L&O*, which helped to improve our manuscript. This work was supported by Agencia Nacional de Promoción Científica y Tecnológica–ANPCyT (PICT 2007-1651), Consejo Nacional de Investigaciones Científicas y Técnicas–Deutsche Forschungsgemeinschaft (CONICET-DFG-2009), Ministerio de Ciencia, Tecnología e Innovación Productiva (MINCyT, Argentina)–Consejo Nacional de Ciencia y Tecnología (CONACYT, Mexico) (MX/09/13), the Dutch Council for Scientific Research (NPP 851.20.031), and Fundación Playa Unión. This is contribution 123 of the Estación de Fotobiología Playa Unión.

References

Beardall, J., C. Sobrino, and S. Stojkovic. 2009. Interactions between the impacts of ultraviolet radiation, elevated CO_2, and nutrient limitation on marine primary producers. Photochem. Photobiol. Sci. **8:** 1257–1265, doi:10.1039/b9pp00034h

Behrenfeld, M. J., and others. 2006. Climate-driven trends in contemporary ocean productivity. Nature **444:** 752–755, doi:10.1038/nature05317

Beisner, B. E., E. McCauley, and F. J. Wrona. 1997. The influence of temperature and food chain length on plankton predator-prey dynamics. Can. J. Fish. Aquat. Sci. **54:** 586–595.

Bergmann, T., T. L. Richardson, H. W. Paerl, J. L. Pinckney, and O. Schofield. 2002. Synergy of light and nutrients on the photosynthetic efficiency of phytoplankton populations from the Neuse River Estuary, North Carolina. J. Plankton Res. **24:** 923–933, doi:10.1093/plankt/24.9.923

Bouchard, J. N., M. L. Longhi, S. Roy, D. A. Campbell, and G. Ferreyra. 2008. Interaction of nitrogen status and UVB sensitivity in a temperate phytoplankton assemblage. J. Exp. Mar. Biol. Ecol. **359:** 67–76, doi:10.1016/j.jembe.2008.02.022

———, S. Roy, and D. A. Campbell. 2006. UVB effects on the photosystem II-D1 protein of phytoplankton and natural phytoplankton communities. Photochem. Photobiol. **82:** 936–951, doi:10.1562/2005-08-31-IR-666

Buma, A. G. J., R. J. Visser, W. Van De Poll, V. E. Villafañe, P. J. Janknegt, and E. W. Helbling. 2009. Wavelength-dependent xanthophyll cycle activity in marine microalgae exposed to natural ultraviolet radiation. Eur. J. Phycol. **44:** 515–524, doi:10.1080/09670260902971894

Demming-Adams, B., and W. W. Adams. 1992. Photoprotection and other responses of plants to high light stress. Ann. Rev. Plant Physiol. **43:** 599–626, doi:10.1146/annurev.pp.43.060192.003123

Dubinsky, Z., and N. Stambler. 2009. Photoacclimation processes in phytoplankton: Mechanisms, consequences, and applications. Aquat. Microb. Ecol. **56:** 163–176, doi:10.3354/ame01345

Dunne, R. P. 2010. Synergy or antagonism—interactions between stressors on coral reefs. Coral Reefs **29:** 145–152, doi:10.1007/s00338-009-0569-6

Falkowski, P. G. 1984. Physiological responses of phytoplankton to natural light regimes. J. Plankton Res. **6:** 295–307, doi:10.1093/plankt/6.2.295

Farman, J. C., B. G. Gardiner, and J. D. Shanklin. 1985. Large losses of total ozone in Antarctica reveal seasonal ClOx/NOx interaction. Nature **315:** 207–210, doi:10.1038/315207a0

Figueroa, F. L., and others. 1997. Effects of solar radiation on photoinhibition and pigmentation in the red alga *Porphyra leucosticta*. Mar. Ecol. Prog. Ser. **151:** 81–90, doi:10.3354/meps151081

Finazzi, G., G. N. Johnson, L. Dall'Osto, F. Zito, G. Bonente, R. Bassi, and F. A. Wollman. 2006. Nonphotochemical quenching of chlorophyll fluorescence in *Chlamydomonas reinhardtii*. Biochemistry **45:** 1490–1498, doi:10.1021/bi0521588

Gao, K., Z. Ruan, V. E. Villafañe, J. P. Gattuso, and E. W. Helbling. 2009. Ocean acidification exacerbates the effect of UV radiation on the calcifying phytoplankter *Emiliania huxleyi*. Limnol. Oceanogr. **54:** 1855–1862, doi:10.4319/lo.2009.54.6.1855

Genty, B. E., J. M. Briantais, and N. R. Baker. 1989. Relative quantum efficiencies of the two photosystems of leaves in photorespiratory and non-photorespiratory conditions. Plant Physiol. Biochem. **28:** 1–10, doi:10.1021/bi00427a001

Gerard, V. A., and T. Driscoll. 1996. A spectrophotometric assay for rubisco activity: Application to the kelp *Laminaria saccharina* and implications for radiometric assays. J. Phycol. **32:** 880–884, doi:10.1111/j.0022-3646.1996.00880.x

Guillard, R. R. L., and J. H. Ryther. 1962. Studies of marine planktonic diatoms. I. *Cyclotella nana* Hustedt, and *Detonula confervacea* (Cleve) Gran. Can. J. Microbiol. **8:** 229–239, doi:10.1139/m62-029

Häder, D. P., H. D. Kumar, R. C. Smith, and R. C. Worrest. 2007. Effects of solar UV radiation on aquatic ecosystems and interactions with climate change. Photochem. Photobiol. Sci. **6:** 267–285, doi:10.1039/b700020k

Halac, S., E. García-Mendoza, and A. T. Banaszak. 2009. Ultraviolet radiation reduces the photoprotective capacity of the marine diatom *Phaeodactylum tricornutum* (Bacillariophyceae, Heterokontophyta). Photochem. Photobiol. **85:** 807–815, doi:10.1111/j.1751-1097.2008.00497.x

———, V. E. Villafañe, and E. W. Helbling. 2010. Temperature benefits the photosynthetic performance of the diatoms *Chaetoceros gracilis* and *Thalassiosira weissflogii* when exposed to UVR. J. Photochem. Photobiol. B **101:** 196–205, doi:10.1016/j.jphotobiol.2010.07.003

Harrison, J. W., and R. E. H. Smith. 2009. Effects of ultraviolet radiation on the productivity and composition of freshwater phytoplankton communities. Photochem. Photobiol. Sci. **8:** 1218–1232, doi:10.1039/b902604e

Helbling, E. W., D. E. Pérez, C. D. Medina, M. G. Lagunas, and V. E. Villafañe. 2010. Phytoplankton distribution and photosynthesis dynamics in the Chubut River estuary (Patagonia, Argentina) throughout tidal cycles. Limnol. Oceanogr. **55:** 55–65, doi:10.4319/lo.2010.55.1.0055

Hernández Moresino, R. D., and E. W. Helbling. 2010. Combined effects of UVR and temperature on the survival of crab larvae (Zoea I) from Patagonia: The role of UV-absorbing compounds. Mar. Drugs **8:** 1681–1698, doi:10.3390/md8051681

Holm-Hansen, O., and E. W. Helbling. 1995. Técnicas para la medición de la productividad primaria en el fitoplancton, p. 329–350. *In* K. Alveal, M. E. Ferrario, E. C. Oliveira, and E. Sar [eds.], Manual de métodos ficológicos. Univ. de Concepción. [Techniques for the measurement of primary productivity in phytoplankton.]

———, C. J. Lorenzen, R. W. Holmes, and J. D. H. Strickland. 1965. Fluorometric determination of chlorophyll. J. Cons. Perm. Int. Explor. Mer **30:** 3–15.

———, and B. Riemann. 1978. Chlorophyll *a* determination: Improvements in methodology. Oikos **30:** 438–447, doi:10.2307/3543338

Houghton, J. T., and others. 2001. Climate change 2001: The scientific basis. Cambridge Univ. Press.

Intergovernmental Panel on Climate Change (IPCC). 2007. Climate change 2007: The physical science basis. Contribution of working group I to the fourth assessment report of the Intergovernmental Panel on Climate Change. Cambridge Univ. Press.

Laney, S. R. 2006. Seconds to hour scale photosynthetic responses in marine microalgae. Oregon State Univ.

Lesser, M. P. 1996*a*. Acclimation of phytoplankton to UV-B radiation: Oxidative stress and photoinhibition of photosynthesis are not prevented by UV-absorbing compounds in the dinoflagellate *Prorocentrum micans*. Mar. Ecol. Prog. Ser. **132:** 287–297, doi:10.3354/meps132287

———. 1996*b*. Elevated temperatures and ultraviolet radiation cause oxidative stress and inhibit photosynthesis in symbiotic dinoflagellates. Limnol. Oceanogr. **41:** 271–283, doi:10.4319/lo.1996.41.2.0271

———, P. J. Neale, and J. J. Cullen. 1996. Acclimation of Antarctic phytoplankton to ultraviolet radiation: Ultraviolet-absorbing compounds and carbon fixation. Mol. Mar. Biol. Biotechnol. **5:** 314–325.

Livak, K. J., and T. D. Schmittgen. 2001. Analysis of relative gene expression data using real-time quantitative PCR and the $2^{-\Delta\Delta C_T}$ method. Methods **25:** 402–408, doi:10.1006/meth.2001.1262

Marcoval, M. A., V. E. Villafañe, and E. W. Helbling. 2007. Interactive effects of ultraviolet radiation and nutrient addition on growth and photosynthesis performance of four species of marine phytoplankton. J. Photochem. Photobiol. B **89:** 78–87, doi:10.1016/j.jphotobiol.2007.09.004

Mckenzie, R., P. J. Aucamp, A. Bais, L. O. Björn, M. Ilyas, and S. Madronich. 2011. Ozone depletion and climate change: Impacts on UV radiation. Photochem. Photobiol. Sci. **10:** 182–198, doi:10.1039/c0pp90034f

Olaizola, M., and H. Y. Yamamoto. 1994. Short-term response of the diadinoxanthin cycle and fluorescence yield to high irradiance in *Chaetoceros muelleri* (Bacillariophyceae). J. Phycol. **30:** 606–612, doi:10.1111/j.0022-3646.1994.00606.x

Porra, R. J. 2002. The chequered history of the development and use of simultaneous equations for the accurate determination of chlorophylls *a* and *b*. Photosynth. Res. **73:** 149–156, doi:10.1023/A:1020470224740

Ramakers, C., J. M. Ruijter, R. H. L. Deprez, and A. F. M. Moorman. 2003. Assumption-free analysis of quantitative real-time polymerase chain reaction (PCR) data. Neurosci. Lett. **339:** 62–66, doi:10.1016/S0304-3940(02)01423-4

Roncarati, F., J. W. Rijstenbil, and R. Pistocchi. 2008. Photosynthetic performance, oxidative damage and antioxidants in *Cylindrotheca closterium* in response to high irradiance, UVB radiation and salinity. Mar. Biol. **153:** 965–973, doi:10.1007/s00227-007-0868-9

Rozen, S., and H. Skaletsky. 2000. Primer3 on the WWW for general users and for biologist programmers. Methods Mol. Biol. **132:** 365–386.

Skewgar, E., P. D. Boersma, G. Harris, and G. Caille. 2007. Sustainability: Anchovy fishery threat to Patagonian ecosystem. Science **315:** 45, doi:10.1126/science.1135767

Sobrino, C., and P. J. Neale. 2007. Short-term and long-term effects of temperature on photosynthesis in the diatom *Thalassiosira pseudonana* under UVR exposures. J. Phycol. **43:** 426–436, doi:10.1111/j.1529-8817.2007.00344.x

———, ———, and L. M. Lubián. 2005. Interaction of UV radiation and inorganic carbon supply in the inhibition of photosynthesis: Spectral and temporal responses of two marine picoplankters. Photochem. Photobiol. **81:** 384–393, doi:10.1562/2004-08-27-RA-295.1

Van De Poll, W., A. G. J. Buma, R. J. Visser, P. J. Janknegt, V. E. Villafañe, and E. W. Helbling. 2010. Xanthophyll cycle activity and photosynthesis of *Dunaliella tertiolecta* (Chlorophyceae) and *Thalassiosira weissflogii* (Bacillariophyceae) during fluctuating solar radiation. Phycologia **49:** 249–259, doi:10.2216/PH-08-83.1

Van De Poll, W. H., and A. G. J. Buma. 2009. Does ultraviolet radiation affect the xanthophyll cycle in marine phytoplankton? Photochem. Photobiol. Sci. **8:** 1295–1301, doi:10.1039/b904501e

Van Leeuwe, M. A., L. A. Villerius, J. Roggeveld, R. J. W. Visser, and J. Stefels. 2006. An optimized method for automated analysis of algal pigments by HPLC. Mar. Chem. **102:** 267–275, doi:10.1016/j.marchem.2006.05.003

Vernet, M., and R. C. Smith. 1997. Effects of ultraviolet radiation on the pelagic Antarctic ecosystem, p. 247–265. *In* D. P. Häder [ed.], The effects of ozone depletion on aquatic ecosystems. R. C. Landes.

Villafañe, V. E., E. S. Barbieri, and E. W. Helbling. 2004. Annual patterns of ultraviolet radiation effects on temperate marine phytoplankton off Patagonia, Argentina. J. Plankton Res. **26:** 167–174, doi:10.1093/plankt/fbh011

———, K. Gao, P. Li, and E. W. Helbling. 2007. Vertical mixing within the epilimnion modulates UVR-induced photoinhibition in tropical freshwater phytoplankton from southern China. Freshw. Biol. **52:** 1260–1270, doi:10.1111/j.1365-2427.2007.01762.x

———, P. J. Janknegt, M. De Graaff, R. J. W. Visser, W. H. Van De Poll, A. G. J. Buma, and E. W. Helbling. 2008. UVR-induced photoinhibition of summer marine phytoplankton communities from Patagonia. Mar. Biol. **154:** 1021–1029, doi:10.1007/s00227-008-0993-0

———, K. Sundbäck, F. L. Figueroa, and E. W. Helbling. 2003. Photosynthesis in the aquatic environment as affected by UVR, p. 357–397. *In* E. W. Helbling and H. E. Zagarese [eds.], UV effects in aquatic organisms and ecosystems. Comprehensive Series in Photochemical and Photobiological Sciences. Royal Society of Chemistry.

Weis, E., and A. Berry. 1987. Quantum efficiency of photosystem II in relation to the energy dependent quenching of chlorophyll fluorescence. Biochim. Biophys. Acta **894:** 198–208, doi:10.1016/0005-2728(87)90190-3

Wrona, F. J., T. D. Prowse, J. D. Reist, J. E. Hobbie, L. M. J. Lévesque, and W. F. Vincent. 2006. Climate change effects on aquatic biota, ecosystem structure and function. Ambio **35:** 359–369, doi:10.1579/0044-7447(2006)35[359:CCEOAB]2.0.CO;2

Wu, H., and K. Gao. 2009. Ultraviolet radiation stimulated activity of extracellular carbonic anhydrase in the marine diatom *Skeletonema costatum*. Funct. Plant Biol. **36:** 137–143, doi:10.1071/FP08172

Zar, J. H. 1999. Biostatistical analysis, 4th ed. Prentice Hall.

Associate editor: Wade H. Jeffrey

Received: 27 December 2010
Accepted: 13 April 2011
Amended: 14 April 2011